Original Article

Efficacy and reliability of three-dimensional fusion guidance for fluoroscopic navigation in transarterial embolization for refractory musculoskeletal pain

Lung-Hui Chiang[1,2], Ya-Che Chen[1,2], Guo-Shu Huang[1,2,3], Ting-Fu Huang[1,2], Yung-Chih Sun[1,2], Wei-Chou Chang[1,2], Yi-Chih Hsu[1,2]

[1]Department of Radiology, Tri-Service General Hospital, Taipei, Taiwan; [2]National Defense Medical Center, Taipei, Taiwan; [3]Department of Medical Research, Tri-Service General Hospital, Taipei, Taiwan

Contributions: (I) Conception and design: YC Hsu, LH Chiang, YC Sun, TF Huang; (II) Administrative support: YC Hsu, LH Chiang; (III) Provision of study materials or patients: YC Hsu, LH Chiang; TF Huang; (IV) Collection and assembly of data: YC Hsu, LH Chiang, YC Sun, TF Huang; (V) Data analysis and interpretation: YC Hsu, LH Chiang, YC Sun, TF Huang; (VI) Manuscript writing: All authors; (VII) Final approval of manuscript: All authors.

Correspondence to: Yi-Chih Hsu, MD. Associate Professor, Department of Radiology, Tri-Service General Hospital, National Defense Medical Center, No. 325, Sec. 2, Cheng-Kung Rd., Neihu Dist. 114, Taipei, Taiwan. Email: doc31578@gmail.com.

Background: This study aimed to evaluate the efficacy and reliability of three-dimensional (3D) fusion guidance in roadmapping for fluoroscopic navigation during trans-arterial embolization for refractory musculoskeletal pain (TAE-MSK pain) in the extremities.

Methods: The included research patients were divided into two groups: group A—TAE-MSK pain performed without the use of 3D fusion guidance; group B—TAE-MSK pain performed with the use of 3D fusion guidance for fluoroscopic navigation. We compared the procedure time, radiation dose, visual analogue scale for pain scores, and adverse effects (before and 3 months after TAE-MSK pain) among the two groups. In the group B, we determined the reliability of ideal branch angle for pre-operative non-contrast 3D magnetic resonance angiography (MRA) and intra-operative 3D cone beam computed tomography (CBCT) angiography.

Results: We recruited 65 patients, including 23 males and 42 females (average age 58.20±12.58 years), with 38 and 27 patients in groups A and B. A total of 247 vessels were defined as target branch vessels. Significant changes were observed in the fluoroscopy time which was 32.31±12.39 and 14.33±3.06 minutes, in group A and group B ($P<0.001$), respectively; procedure time, which was 46.45±17.06 in group A and 24.67±9.78 in group B ($P<0.001$); and radiation exposure dose, determined as 0.71±0.64 and 0.34±0.29 mSv ($P<0.01$) in group A and group B, respectively. Furthermore, the number of target branch vessels, that underwent successful catheterization were 107 (97%) in group B as compared to 96 (70%) in group A, which was also significant ($P<0.001$). The study also showed that the ideal branch-angle has a similarly high consistency in pre-operative and intra-operative angiography based on the intra-class correlation coefficient (ICC) (0.994; 0.990, respectively).

Conclusions: 3D fusion guidance for fluoroscopic navigation not only is a reliable process, but also effectively reduces the operation time and radiation dose of TAE-MSK pain.

Keywords: Angiography; fluoroscopic navigation; magnetic resonance; musculoskeletal pain; trans-arterial embolization

Submitted Apr 12, 2023. Accepted for publication Aug 11, 2023. Published online Sep 12, 2023.
doi: 10.21037/qims-23-490
View this article at: https://dx.doi.org/10.21037/qims-23-490

© Quantitative Imaging in Medicine and Surgery. All rights reserved.

Introduction

Transarterial embolization (TAE) is a widely used treatment for aggravating musculoskeletal pain (MSK pain) in the extremities, that is refractory to conservative treatment or to percutaneous injections (1-5). Under normal circumstances, visualization of arterial branches with staining of abnormal vessels, which should be targeted in TAE for pain control is guided by two-dimensional (2D) angiography (2,4,5). Detailed information from the staining of abnormal target vessels is essential for successful catheterization and sufficient TAE (2-5). However, it is sometimes difficult to identify some extremity arteries on 2D angiographic images because of overlapping vessels.

Three-dimensional (3D) cone-beam computed tomography (CBCT) technology using a flat-panel detector during angiography, has shown good 3D angiography and cross-sectional soft tissue imaging as part of the angiography system (6). 3D-CBCT is a technique that permits assessment of complex vascular anatomy of the area of interest and the complex arterial navigation further helps for road-mapping during complex arterial catheterization (6-8). As compared to conventional radiography, CBCT has an added advantage for MSK disorders due to its high spatial resolution resulting in intense details of bone microarchitecture (9). Intraoperative fluoroscopy alone, may be less sensitive to identify potential lesions, and also may require higher cumulative dose and longer time (10). The use of CBCT guidance along with fluoroscopy can aid in choosing the best approach, track and detect errors in the operating room, further helping to reduce the fluoroscopy time (11).

Fusion imaging is a technique that involves 3D visualization of structures by fusion of preoperative 3D CBCT images into intraoperative 2D fluoroscopy images (2D-3D fusion imaging) (12). Multimodality image fusion guidance could be the next new alternative to conventional angiogram road-mapping in endovascular procedures, which can effectively facilitate the vascular embolization and reduce radiation dose (13,14). Previous research demonstrated the feasibility of image fusion of pre-angiography 3D contrast CT and magnetic resonance angiography (MRA) with intra-procedural fluoroscopy for road-mapping in endovascular treatment of aortoiliac steno-occlusive disease (14). However, there has been limited exploration of this technique for visualization of blood vessels in the extremities. The usefulness of 2D/3D registration has been previously illustrated during hip joint and femur fluoroscopy procedures (10,15).

The purpose of this study was to evaluate the efficacy of 3D fusion guidance for fluoroscopic navigation in TAE for refractory MSK pain (TAE-MSK pain). We assessed the efficacy based on the detection and successful catheterization of the target vessels. We also aimed to assess the reliability and safety of pre-procedural non-contrast 3D MRA and intra-operative 3D CBCT angiography during road-mapping for fluoroscopy procedure. We determined this reliability of ideal branch-angle by measuring the included angle for ideal separating of the target vessel branch from the main trunk artery in the key 2D reference images and roadmap images for navigation use.

Methods

Patients

This retrospective study was conducted in accordance with the Declaration of Helsinki (as revised in 2013). The study was approved by institutional review board of Tri Service General Hospital and individual consent for this retrospective analysis was waived. Patients were included based on the following criteria: (I) diagnosed with either osteoarthritis of knee (2); adhesive capsulitis of shoulder (5); and tendinopathy or enthesopathy confirmed by physical examination or ultrasound-guided provocation injection regardless of location (1). (II) Underwent previous conservative therapies (rest, anti-inflammatory drugs, ice, stretching, strengthening, corticosteroid injections, and physical therapy) applied for at least 3 months, and persistent moderate to severe pain [i.e., visual analog scale (VAS) score >50] (1,2,5). Patients were excluded from the study if they had reported local infection, tumor, bleeding tendency, and restless limb.

The patients with clinically suspected refractory MSK pain were evaluated by the interventional radiologist who further considered the procedures conducted between November 2020 and December 2021. We included 67 patients, who received TAE for refractory MSK pain (*Figure 1*). We excluded 2 patients who could not complete the TAE and with a restless limb to perform CBCT because the images were not clear. Therefore, this study finally included a total of 65 patients with 23 males and 42 females, in the age range of 42-to-84 years old.

The included research patients were divided into two groups: group A—TAE-MSK pain performed without the use of 3D fusion guidance for fluoroscopic navigation;

© Quantitative Imaging in Medicine and Surgery. All rights reserved.

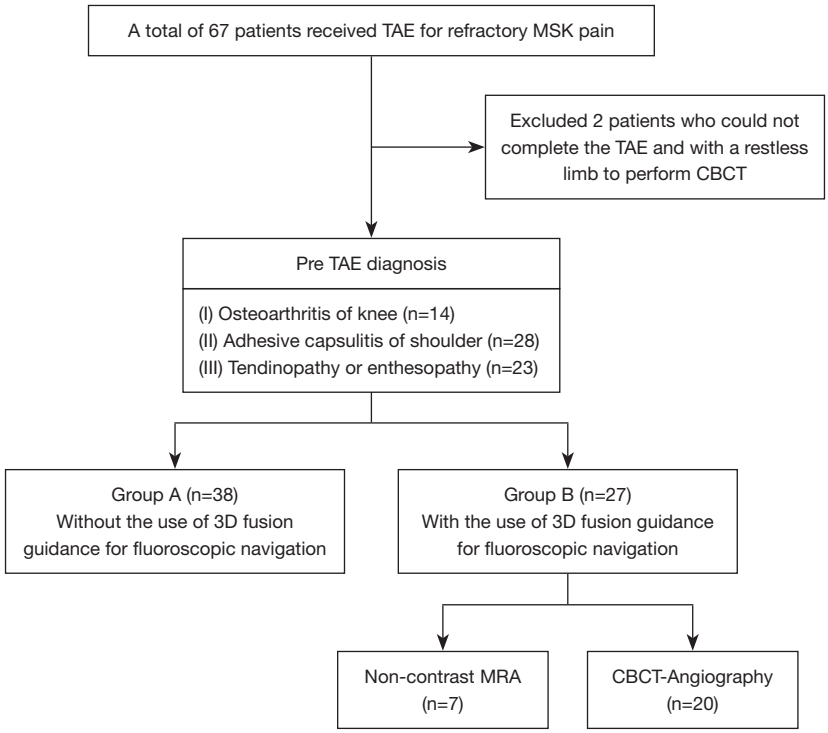

Figure 1 Flowchart illustrating patient selection for the study. TAE, transarterial embolization; MSK, musculoskeletal; CBCT, cone bean computed tomography; MRA, magnetic resonance angiography.

group B—TAE-MSK pain performed with the use of 3D fusion guidance for fluoroscopic navigation during the procedure (with an aim to overcome the difficulty of overlapping vessels).

Procedure

All MSK-TAE pain procedures, for patients in both the groups, were carried out by an interventional radiologist with 15 years' experience. The femoral artery or radial artery was selected to perform puncture in an ipsilateral antegrade fashion for the TAE procedure using a commercial ceiling angiography system (Siemens Artis Q system, Siemens Healthcare, Forchheim, Germany). Arterial access was gained percutaneously by using a 5-Fr sheath (Terumo, Tokyo, Japan) under ultrasound-guidance. After the intravenous administration of 2,000 IU heparin sodium (Mitsubishi Tanabe, Osaka, Japan), a 5-Fr angiographic catheter was inserted towards the target lesion and a 2.4-Fr microcatheter (Merit maestro) was inserted coaxially through the 5-Fr catheter to be selectively placed in the targeted branch arteries.

For the patients in group B, we further observed the two types of 3D imaging techniques used for subsequent fusion guidance and fluoroscopic navigation—non-contrast MRA, which was performed prior TAE-MSK pain; and CBCT angiography, performed during TAE-MSK pain procedure. Protocol of non-contrast MRA and CBCT angiography have been described in *Table 1*. Pre-procedural non-contrast MRA has been one of the routinely performed procedures in our hospital for TAE-MSK pain in upper extremities, since CBCT has a fixed field of view, more suitable for visceral organs and lower extremities (8). However, majority of our patients required TAE-MSK pain for lower extremities and subsequently, intra-procedural CBCT angiography was conducted for the other remaining patients in group B. For those patients who underwent pre-TAE non-contrast MRA procedure, the available images were imported to the 3D workstation (syngo X Workplace, Siemens Healthcare, Forchheim, Germany) for planning and image fusion. Two intraoperative 2D projections, including one anteroposterior 2D-digital subtraction angiography and the other with roadmap at least 30 degrees apart, were used for 2D/3D image registration (syngo 2D-3D fusion,

© Quantitative Imaging in Medicine and Surgery. All rights reserved.

Table 1 Protocol of non-contrast MRA and CBCT angiography

	Non-contrast MRA	CBCT angiography
Instrument	GE/signa PET-MR 750W 3T	Siemens/artis Q
Protocols	Non contrast gated 3D-FSE MRA	Acquisition time: 5 s
	Inhance deltaflow:	kV: 90–96 kV
	Acquisition time: 4.36 s	Matrix: 512×512
	Acquisition number: 1	Frame: 395–397
	TE: 80 s	0.5°/frame
	Frequency × phase: 320×224	Total angle: 200°
	FOV: 30 cm	Detector size: 30 cm × 40 cm
	Trigger type: PG	Injector rate: 2 mL/s
		Total volume: 20 mL
		X-ray delay time: 4 s
		Contrast: saline =5:2

MRA, magnetic resonance angiography; CBCT, cone bean computed tomography; PET-MR, positron emission tomography-magnetic resonance; FSE, fast spin-echo; TE, time to echo; FOV, field of view; PG, peripheral gated.

Siemens Healthcare, Forchheim, Germany) automatically on the 3D workstation (16). For the other patients in group B, undergoing CBCT-angiography, images were acquired intraoperatively using flat-panel interventional angiography system (Siemens Artis Q ceiling) and software (5-second syngo DynaCT, Siemens Healthcare, Forchheim, Germany). Thereafter, interventional radiologists determined the ideal target branch vessel branch separated from main trunk artery on the 3D workstation and the saved key 2D reference image. C-arm gantry was then automatically positioned depending on the reference image selected (syngo Automap, Siemens Healthcare, Forchheim, Germany), following by creating and saving one roadmap for later navigation use (*Figure 2*) (17). After confirming that the abnormal staining, which was the characteristic for determining of target branch vessels (1,2,5), TAE-MSK pain was performed cautiously injecting 0.1–0.3 mL of the embolic agent at a time using a 3 mL syringe. A suspension of embosphere (particle size: 100–300 μm) (Ems; Biosphere Medical, Rockland, USA) mixed with iodinated contrast medium was used as an embolic agent. The aim of TAE-MSK pain procedure was to "prune" the abnormal vessels and maintain the larger native artery branches (2).

Data collection and analysis

Efficacy assessment included the detection of the target vessels and target vessel catheterization during TAE. Reliability was assessed based on difference of the included angle "Θ" between the key 2D reference images and roadmap images for navigation use. Safety evaluation was based on the radiation dose and the occurrence of adverse events.

Clinical data including sex, age, regions of TAE-MSK pain, the number of target branch vessels for TAE-MSK pain, number of overlapping target branch vessels for TAE-MSK pain, number of separating target branch vessels for TAE-MSK pain and the number of target branch vessels that successfully underwent catheterization of target branch vessels were routinely recorded for patients in both the groups. We also assessed the procedure time, radiation doses, VAS scores, and adverse effects (before and 3 months after TAE-MSK pain procedure). The change in the VAS (ΔVAS) scores of the patients was defined as the difference between the baseline and 3 months after TAE-MSK pain procedure. Dose report of each case after treatment was used to evaluate the radiation exposure dose and the total fluoroscopy time. With regards to the radiation exposure of the patients suffering from TAE-MSK pain, we noted the effective dose, which has been generally accepted as a single number index reflecting patient radiation risk. It was subsequently calculated using the latest International Commission on Radiological Recommendations 103 weighing factors, published in 2007 (18). The physician's exposure dose is monitored by a personnel film. The personnel film records the radiation dose for a period of one month, making it difficult to read the accurate medical exposure dose for a single operation.

The above-mentioned key 2D reference images from image fusion results by either non-contrast MRA or CBCT angiography and the roadmap images for navigation use were retrieved from Picture Archiving and Communication System for measuring the angle for ideal separation of the target vessel branch from the main trunk artery. Two senior interventional radiology technologists measured the included angle "Θ" between target branch vessel branch and main trunk (*Figure 3*) in the saved images of each patient and were blinded to measure the included angle of all images. Duplicate measurements were taken and recorded by each rater at a regular interval of two weeks.

© Quantitative Imaging in Medicine and Surgery. All rights reserved.

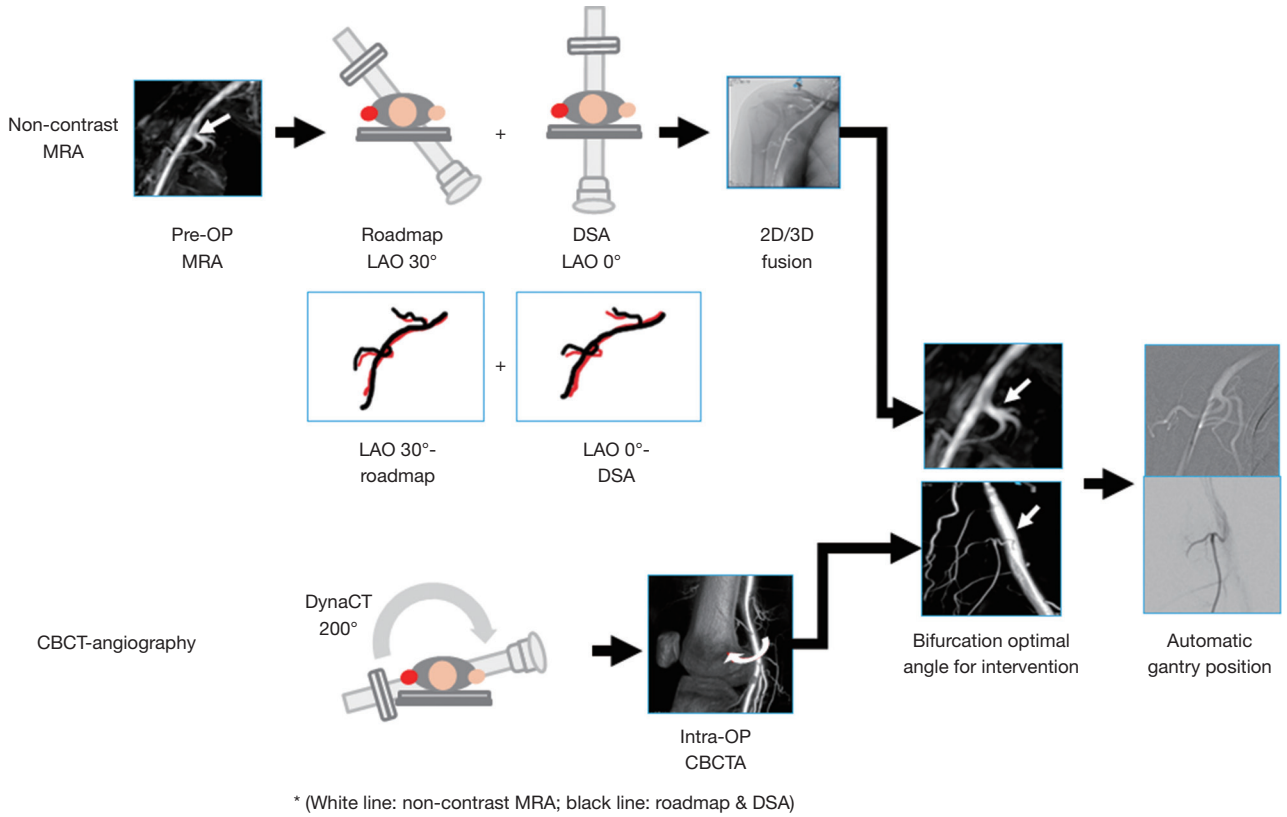

Figure 2 The three-dimensional image fusion techniques used in fluoroscopic navigation. The processes for the pre-operative non-contrast 3D MRA and 3D CBCT angiography for 3D image fusion used in fluoroscopic navigation among group B patients. The 3D image was rotated in the workstation to obtain the easiest separation angle between the target vessel and the main trunk. The workflow indicates how the ideal target branch vessel was separated from main trunk artery on the 3D workstation and the saved key 2D reference image. White arrows indicate target vessels. Group B: TAE-MSK pain performed with the use of 3D fusion guidance for fluoroscopic navigation. MRA, magnetic resonance angiography; OP, operative; LAO, left anterior oblique; DSA, digital subtraction angiography; CBCT, cone bean computed tomography; CT, computed tomography; CBCTA, cone bean computed tomography angiography.

The mean of the repeated measurements was used as the final value (19).

Statistical analysis

All measurements of changes in the two groups (age, VAS scores, fluoroscopy time, etc.) were presented as means ± standard deviation. Differences in baseline characteristics between the two groups were compared using a chi-square test and a Mann-Whitney *U* test. Intra-class correlation coefficient (ICC) of the ideal branch-angle for fluoroscopic navigation was used to analyze the consistency of the difference in the included angle "Θ" between the key 2D reference images and roadmap images for navigation use. Statistically significant differences were defined by a P value <0.05. All statistical data were analyzed using the SPSS software (IBM SPSS Statistics for Windows, Version 22.0. Armonk, NY, USA: IBM Corp.).

Results

The baseline characteristics of the study cohort are detailed in *Table 2*. Group A comprised of 38 patients, 13 males and 25 females, who underwent TAE without the use of 3D fusion guidance for fluoroscopic navigation. Group B constituted 27 patients, 10 males and 17 females, who underwent TAE with the use of 3D fusion guidance for fluoroscopic navigation (*Figure 1*). In group A, there were 21 patients (55%) treated for MSK pain in upper extremities, and 17 patients (45%) for pain in lower extremities; while in

© Quantitative Imaging in Medicine and Surgery. All rights reserved.

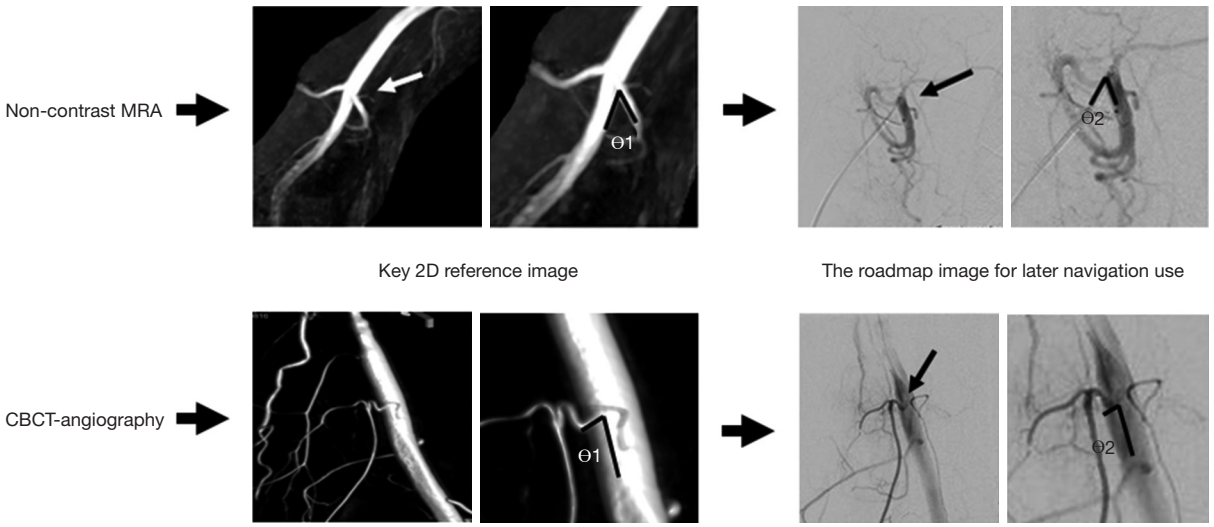

Figure 3 Evaluating the reliability of image fusion for fluoroscopic navigation based on the measurement of the included angle before and after fusion. (Remarks: the measurement method is based on the angle between the long axis of the main vessel wall and the long axis of the target branch vessel as the measurement benchmark). Black arrows and white arrows: target branch vessel. Θ1: angle measured in the key 2D reference image; Θ2: angle measured after fusion of 2D reference image and roadmap image. MRA, magnetic resonance angiography; CBCT, cone bean computed tomography.

Table 2 Baseline characteristics of the study cohort

Variable	Group A (N=38)	Group B (N=27)	P value
Sex			
Male	13 (34%)	10 (37%)	0.814
Female	25 (66%)	17 (63%)	
Age (years)	59.16±12.01	57.85±13.63	0.684
Region			
Upper extremity	21 (55%)	7 (26%)	
Lower extremity	17 (45%)	20 (74%)	
Total number of target branch vessels	137	110	
Number of target branch vessels per patient	(3 to 5) ±1.20	(2 to 6) ±1.42	0.157
Total number of overlapping target branch vessels	33 (24%)	22 (20%)	0.443
Total number of target branch vessels catheterized	96 (70%)	107 (97%)	<0.001

Data are presented as mean ± standard deviation/N (%). Group A: patients without the use of 3D fusion guidance for fluoroscopic navigation; Group B: patients with the use of 3D fusion guidance for fluoroscopic navigation.

group B, 7 patients (26%) received treatment for MSK pain in the upper extremities, and 20 patients (74%) for pain in lower extremities (*Table 2*). Among the patients treated for pain in lower extremities, one patient in group A and two patients in group B had previously undergone total knee arthroplasty. There were no major adverse events related to the procedures. Minor adverse effects such as puncture site hematoma/pain/skin color change were observed during the follow-up after the procedure.

Regarding the discomfort of the patients, the VAS scores

© Quantitative Imaging in Medicine and Surgery. All rights reserved.

Table 3 The differences in VAS scores, fluoroscopy time and effective radiation dose between groups A and B

Variable	Group A	Group B	P value
VAS scores			
Before TAE-MSK pain	7.87±1.49	7.52±1.48	0.353
After TAE-MSK pain	3.08±2.83	2.63±2.90	0.535
ΔVAS scores	4.79±2.60	4.89±2.69	0.882
Fluoroscopy time (min)	32.31±12.39	14.33±3.06	<0.001*
Procedure time (min)	46.45±17.06	24.67±9.78	<0.001*
Effective radiation dose (mSv)	0.71±0.64	0.34±0.29	<0.01*

Data are presented as mean ± standard deviation. *, P<0.01, statistically significant. Group A: patients without the use of 3D fusion guidance for fluoroscopic navigation; Group B: patients with the use of 3D fusion guidance for fluoroscopic navigation; VAS, visual analogue scale; TAE-MSK, transarterial embolization for refractory musculoskeletal pain.

Table 4 Observation between non-contrast 3D MRA and 3D CBCT angiography among group B patients

Variable	Non-contrast 3D MRA	3D CBCT angiography	P value
Number of patients	7	20	
Total number of target branch vessels	28	82	
Number of target branch vessels per patient	(2 to 4) ±0.22	(3 to 5) ±1.12	0.191
Total number of overlapping target branch vessels for TAE	4 (14%)	18 (22%)	0.381
Total number of separating target branch vessels for TAE after 3D fusion guidance	28 (100%)	82 (100%)	1
Number of target branch vessels selectively catheterized	28 (100%)	78 (95%)	0.234
Difference of included angle between main trunk and target branch artery (degree)	2.29±1.18	2.78±1.26	0.378
ICC	0.994	0.990	

Data are presented as mean ± standard deviation/N (%). MRA, magnetic resonance angiography; CBCT, cone beam computed tomography; TAE, transarterial embolization; ICC, intraclass correlation coefficient.

before TAE (group A: 7.87±1.49, group B: 7.52±1.48; P=0.353) decreased 3 months after TAE (group A: 3.08±2.83, group B: 2.63±2.90) but there were no significant intergroup differences (P=0.535). The ΔVAS scores of group A and B were 4.79±2.60 and 4.89±2.69, respectively, with no statistical significance between the two groups (P=0.882). The total fluoroscopy time during the TAE procedure in the group A and group B was 32.31±12.39 and 14.33±3.06 minutes (P<0.001) and the procedure time also reduced by 46.8% (P<0.001). The cumulative effective dose in group A and group B were 0.71±0.64 and 0.34±0.29 mSv (P<0.01), reduced approximately by 52.1% in group B. Both fluoroscopy time and effective radiation dose showed a statistically significant reduction in group B as compared to group A (*Table 3*).

In group B, using 3D fusion guidance for fluoroscopic navigation, we also determined the difference of the included angle "Θ" between the key 2D reference images and roadmap images for navigation use. *Table 4* shows the findings for non-contrast 3D MRA (n=7) and 3D CBCT-angiography (n=20) among the patients in group B (n=27), with 28 and 82 target branch vessels, respectively. The number of overlapping target branch vessels for TAE-MSK pain were 4 vessels (14%) for 3D MRA and 18 vessels (22%) for 3D CBCT angiography (P=0.381). The number of separating target branch vessels for TAE after 3D fusion guidance were 28 vessels (100%) for 3D MRA and 82 vessels (100%) for 3D CBCT angiography. For non-contrast 3D MRA, there were 28 vessels (100%) that were successfully catheterized; while in patients who underwent 3D CBCT

© Quantitative Imaging in Medicine and Surgery. All rights reserved.

angiography, 78 vessels (95%) were successfully treated by catheterization of target branch vessels, and 4 vessels (5%) could not complete the catheterization due to the implants used for total knee arthroplasty among 2 patients. The differences of measured included angle between main trunk and target branch artery were 2.94±1.18 degrees for 3D MRA and 2.78±1.26 degrees for 3D CBCT angiography, and the 3D image angle showed a higher consistency of ideal branch-angle for fluoroscopic navigation based on ICC values 0.994 and 0.990, respectively.

Discussion

This study demonstrated the efficacy, reliability and safety of the use of 3D fusion guidance in comparison to the procedure without the use of 3D fusion guidance for fluoroscopic navigation in TAE for refractory MSK pain. The key to performing a successful TAE is the safe and effective catheterization of the target vessels with the tip of the angiocatheter. Our data showed that 3D fusion guidance was effective and reliable for the interventionist in the catheterization of target branch vessels during the TAE. Furthermore, there was also a significant reduction in fluoroscopy time and effective radiation dose. The fusion imaging combining CBCT, and fluoroscopic navigation helps to efficiently guide the procedure, decide the best approach, and identify errors in the operating room, thus lowering the overall procedure time and radiation dose exposure. Therefore, we suggest that 3D fusion guidance can be considered as a supplemental technique in TAE for refractory MSK pain.

This study also observed the two types of 3D imaging processes used for subsequent fusion guidance and fluoroscopic navigation, namely, the pre-operative 3D MRA and the intra-operative 3D CBCT angiography. Although a previous study demonstrated that fluoroscopic navigation using 3D-CBCT for prostatic artery embolization can facilitate catheterization by morphologically identifying prostate arteries (8), quantitative measure of the reliability of this fluoroscopic navigation was not done. Our study mainly focused on the analysis of the reliability of trajectory by the branch-angle differences of main trunk and target branch artery, rather than differences in vessels location, despite the two types of 3D imaging processes being performed on upper and lower extremities, respectively. Herein, we measured the reliability of fluoroscopic navigation by determining the difference of the included angle "Θ" between the key 2D reference images and roadmap images for navigation use. The study also showed that non-contrast 3D magnetic resonance before TAE has high consistency of the ideal branch-angle similar to that of intra-operative CBCT angiography for fluoroscopic navigation. Although the image quality of non-contrast 3D MRA needs to be carefully adjusted, it has more advantages. For example, it can be done before angiography, with no radiation, no contrast agent, and can achieve the position that CBCT cannot, especially for TAE in shoulder (20). Therefore, non-contrast 3D MR before TAE is a viable alternative to CBCT angiography for fluoroscopic navigation.

CBCT has recently been adapted for use with C-arm systems. This configuration provides projection radiography, fluoroscopy, digital subtraction angiography, and volumetric CT capabilities in a single patient setup, within the interventional suite (21). Such capabilities allow the physician to perform 3D imaging during TAE without the need for patient transportation. Although additional radiation dose of CBCT during TAE cannot be avoided, judicious use of in-suite CBCT may reduce patient dose by providing critical diagnostic information, thereby avoiding the need for excessive fluoroscopy. Moreover, considering the limited field-of-view to the anatomic area of interest for minimizing the patient dose and avoiding the C-arm hitting the patient, CBCT can be applied only to visceral organs of trunk (21,22). This also limits the use of CBCT in 3D fusion guidance for navigation in TAE for refractory MSK of upper extremities.

Similar to our findings, previous reports have demonstrated that it is feasible to use 3D contrast CT angiography and 3D contrast MRA for fluoroscopic navigation (14,16). There is no significant difference in the morphology of blood vessels as observed in non-contrast 3D MRA and contrast MRA (23). Hence, non-contrast 3D MRA is a viable alternative to 3D contrast-MRA with additional advantage of lower probability of gadolinium-based toxicity of contrast agents. To our knowledge, this was the first study to quantify the measures and suggest adoption of the non-contrast 3D MRA, as an examination performed before TAE for refractory MSK pain, for fluoroscopic navigation during TAE.

Chau *et al.* (24) demonstrated that TAE may be a treatment option for persistent unexplained pain after total knee arthroplasty, which occurred in approximately 20% of patients who underwent total knee arthroplasty (25). Unlike

© Quantitative Imaging in Medicine and Surgery. All rights reserved.

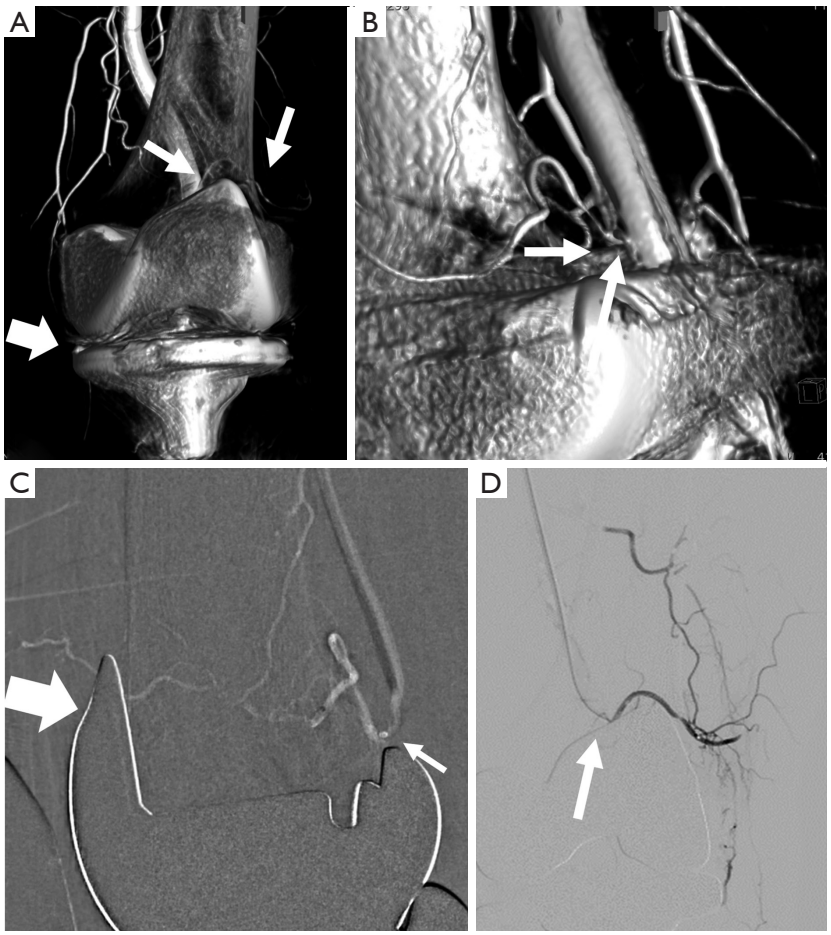

Figure 4 Case example. A 70-year-old female, with history of refractory right knee pain after total knee arthroplasty one year ago and underwent TAE. The 3D-CBCT angiography image revealed the target branch vessel—medial superior genicular artery, the orifice of which was invisible due to overlapping and being obscured by the metal implant used in the total knee arthroplasty at anteroposterior projection (A). The target branch vessel can be separated from popliteal artery and is clearly visible at the best viewing angle (LAO 105°/CRAN 90°) on adjusting the 3D-CBCT angiography image at the workstation (B). After 3D fusion guidance for fluoroscopic navigation, the target branch vessel can be identified without overlapping on roadmap image at the automatic gantry position (C). Successful catheterization of the target branch vessel on digital subtraction image at anteroposterior projection (D). Thin white arrow: target vessel; thick white arrow: metal implant. TAE, transarterial embolization; CBCT, cone bean computed tomography; LAO, left anterior oblique; CRAN, cranial.

intraoperative CBCT angiography, which is a feasible technique for the anatomic area of interest status post implant fixations (26), non-contrast 3D MRA cannot be successfully completed due to metallic artifacts. In our study, CBCT angiography could accurately assess the complex vascular anatomy, which could not be clearly distinguished on fluoroscopy due to the presence of implant which also prevented catheterization of target branch vessels during 3D fusion guidance for fluoroscopic navigation (example shown in *Figure 4A-4D*). Intraoperative CBCT angiography may be the only option during 3D fusion guidance for fluoroscopic navigation in patients with implant fixation at the area of interest. Even so, we still could not completely dodge the metallic implant to achieve successful target branch vessel catheterization on fluoroscopy in all our patients with similar condition.

This study had some limitations. Firstly, its retrospective design and a relatively small number of patients, which inherently decreased the statistical strength. Further studies using this technique with a larger number of patients

© Quantitative Imaging in Medicine and Surgery. All rights reserved.

are warranted. Secondly, the case number was unevenly distributed between upper and lower extremities. However, the study aimed to investigate the application of 3D imaging technology and fusion accuracy on target vessels rather than the anatomic area of interest. Future research could be aimed towards improvement of the uniformity of a single site. Thirdly, a possible technical limitation is that breathing may affect the static status of the anatomic area of interest, potentially causing overlay inaccuracy during the 3D fusion guidance for fluoroscopic navigation (22). Fortunately, the indications of TAE-MSK pain in this study are in the limbs, which are relatively static. Furthermore, TAE-MSK pain using 3D fusion guidance was observed for different parts of the body, which may imply different levels of difficulty in target arterial catheterization. We noticed a similarity in the number of target vessels identified in each patient (*Table 4*), whether the procedure was performed in the upper or lower extremities. Moreover, the variation in radiation dose, has been previously related to the number of images taken, which in turn depends upon the number of target vessels to be catheterized, and not influenced by the site (27).

In conclusion, 3D fusion guidance for fluoroscopic navigation could be reliable and contributes to the effectiveness of TAE for refractory MSK pain despite the inclusion of patients with overlapping vessels. In addition, non-contrast 3D MR before TAE is a reasonable alternative for patients who are probably not candidates for CBCT during TAE. Further experience with larger number of patients is required to determine the utmost utility of this technique.

Acknowledgments

The authors thank the Siemens Healthcare Frank Chun-Hsien Wu and Shwetambara Malwade for their expertise and technical assistance.
Funding: None.

Footnote

Conflicts of Interest: All authors have completed the ICMJE uniform disclosure form (available at https://qims.amegroups.com/article/view/10.21037/qims-23-490/coif). The authors have no conflicts of interest to declare.

Ethical Statement: The authors are accountable for all aspects of the work in ensuring that questions related to the accuracy or integrity of any part of the work are appropriately investigated and resolved. The study was conducted in accordance with the Declaration of Helsinki (as revised in 2013). The study was approved by institutional review board of Tri Service General Hospital and individual consent for this retrospective analysis was waived.

Open Access Statement: This is an Open Access article distributed in accordance with the Creative Commons Attribution-NonCommercial-NoDerivs 4.0 International License (CC BY-NC-ND 4.0), which permits the non-commercial replication and distribution of the article with the strict proviso that no changes or edits are made and the original work is properly cited (including links to both the formal publication through the relevant DOI and the license). See: https://creativecommons.org/licenses/by-nc-nd/4.0/.

References

1. Okuno Y, Matsumura N, Oguro S. Transcatheter arterial embolization using imipenem/cilastatin sodium for tendinopathy and enthesopathy refractory to nonsurgical management. J Vasc Interv Radiol 2013;24:787-92.
2. Little MW, Gibson M, Briggs J, Speirs A, Yoong P, Ariyanayagam T, Davies N, Tayton E, Tavares S, MacGill S, McLaren C, Harrison R. Genicular artEry embolizatioN in patiEnts with oSteoarthrItiS of the Knee (GENESIS) Using Permanent Microspheres: Interim Analysis. Cardiovasc Intervent Radiol 2021;44:931-40.
3. Torkian P, Golzarian J, Chalian M, Clayton A, Rahimi-Dehgolan S, Tabibian E, Talaie R. Osteoarthritis-Related Knee Pain Treated With Genicular Artery Embolization: A Systematic Review and Meta-analysis. Orthop J Sports Med 2021;9:23259671211021356.
4. Bagla S, Piechowiak R, Hartman T, Orlando J, Del Gaizo D, Isaacson A. Genicular Artery Embolization for the Treatment of Knee Pain Secondary to Osteoarthritis. J Vasc Interv Radiol 2020;31:1096-102.
5. Hwang JH, Park SW, Kim KH, Lee SJ, Oh KS, Chung SW, Moon SG. Early Results of Transcatheter Arterial Embolization for Relief of Chronic Shoulder or Elbow Pain Associated with Tendinopathy Refractory to Conservative Treatment. J Vasc Interv Radiol 2018;29:510-7.
6. Fernández Martínez AM, Baldi S, Alonso-Burgos A, López R, Vallejo-Pascual ME, Cuesta Marcos MT, Romero Alonso D, Rodríguez Prieto J, Mauriz JL. Mid-

© Quantitative Imaging in Medicine and Surgery. All rights reserved.

Term Results of Transcatheter Arterial Embolization for Adhesive Capsulitis Resistant to Conservative Treatment. Cardiovasc Intervent Radiol 2021;44:443-51.
7. Okuno Y, Iwamoto W, Matsumura N, Oguro S, Yasumoto T, Kaneko T, Ikegami H. Clinical Outcomes of Transcatheter Arterial Embolization for Adhesive Capsulitis Resistant to Conservative Treatment. J Vasc Interv Radiol 2017;28:161-7.e1.
8. Minami Y, Yagyu Y, Murakami T, Kudo M. Tracking Navigation Imaging of Transcatheter Arterial Chemoembolization for Hepatocellular Carcinoma Using Three-Dimensional Cone-Beam CT Angiography. Liver Cancer 2014;3:53-61.
9. Padia SA, Genshaft S, Blumstein G, Plotnik A, Kim GHJ, Gilbert SJ, Lauko K, Stavrakis AI. Genicular Artery Embolization for the Treatment of Symptomatic Knee Osteoarthritis. JB JS Open Access 2021;6:e21.00085.
10. Kakeda S, Korogi Y, Ohnari N, Moriya J, Oda N, Nishino K, Miyamoto W. Usefulness of cone-beam volume CT with flat panel detectors in conjunction with catheter angiography for transcatheter arterial embolization. J Vasc Interv Radiol 2007;18:1508-16.
11. Miyayama S, Yamashiro M, Okuda M, Yoshie Y, Sugimori N, Igarashi S, Nakashima Y, Matsui O. Usefulness of cone-beam computed tomography during ultraselective transcatheter arterial chemoembolization for small hepatocellular carcinomas that cannot be demonstrated on angiography. Cardiovasc Intervent Radiol 2009;32:255-64.
12. Cadour F, Tradi F, Habert P, Scemama U, Vidal V, Jacquier A, Bartoli JM, Moulin G, Bessayah A. Prostatic artery embolization using three-dimensional cone-beam computed tomography. Diagn Interv Imaging 2020;101:721-5.
13. Posadzy M, Desimpel J, Vanhoenacker F. Cone beam CT of the musculoskeletal system: clinical applications. Insights Imaging 2018;9:35-45.
14. Ku PC, Martin-Gomez A, Gao C, Grupp R, Mears SC, Armand M. Towards 2D/3D Registration of the Preoperative MRI to Intraoperative Fluoroscopic Images for Visualization of Bone Defects. Comput Methods Biomech Biomed Eng Imaging Vis 2023;11:1096-105.
15. Kroes MW, Busser WM, Hoogeveen YL, de Lange F, Schultze Kool LJ. Laser Guidance in C-Arm Cone-Beam CT-Guided Radiofrequency Ablation of Osteoid Osteoma Reduces Fluoroscopy Time. Cardiovasc Intervent Radiol 2017;40:728-34.
16. Schulz CJ, Schmitt M, Böckler D, Geisbüsch P. Feasibility and accuracy of fusion imaging during thoracic endovascular aortic repair. J Vasc Surg 2016;63:314-22.
17. Abi-Jaoudeh N, Kobeiter H, Xu S, Wood BJ. Image fusion during vascular and nonvascular image-guided procedures. Tech Vasc Interv Radiol 2013;16:168-76.
18. Ierardi AM, Duka E, Radaelli A, Rivolta N, Piffaretti G, Carrafiello G. Fusion of CT Angiography or MRA with Unenhanced CBCT and Fluoroscopy Guidance in Endovascular Treatments of Aorto-Iliac Steno-Occlusion: Technical Note on a Preliminary Experience. Cardiovasc Intervent Radiol 2016;39:111-6.
19. Grupp RB, Unberath M, Gao C, Hegeman RA, Murphy RJ, Alexander CP, Otake Y, McArthur BA, Armand M, Taylor RH. Automatic annotation of hip anatomy in fluoroscopy for robust and efficient 2D/3D registration. Int J Comput Assist Radiol Surg 2020;15:759-69.
20. Schwein A, Chinnadurai P, Behler G, Lumsden AB, Bismuth J, Bechara CF. Computed tomography angiography-fluoroscopy image fusion allows visceral vessel cannulation without angiography during fenestrated endovascular aneurysm repair. J Vasc Surg 2018;68:2-11.
21. Wei W, Schön N, Dannenmann T, Petzold R. Determining the position of a patient reference from C-Arm views for image guided navigation. Int J Comput Assist Radiol Surg 2011;6:217-27.
22. The 2007 Recommendations of the International Commission on Radiological Protection. ICRP publication 103. Ann ICRP 2007;37:1-332.
23. Hsu YC, Yang FC, Hsu HH, Huang GS. Schädigung des N. medianus bei ultraschallgesteuerter Hydrodissektion und Kortikosteroid-Injektionen bei Karpaltunnelsyndrom. Ultraschall Med 2022;43:e12.
24. Chau Y, Roux C, Breuil V, Trojani C, Gonzalez JF, Amoretti N, Sédat J. Endovascular Occlusion of Neovascularization as a Treatment for Persistent Pain After Total Knee Arthroplasty. Cardiovasc Intervent Radiol 2020;43:787-90.
25. Orth RC, Wallace MJ, Kuo MD; Technology Assessment Committee of the Society of Interventional Radiology. C-arm cone-beam CT: general principles and technical considerations for use in interventional radiology. J Vasc Interv Radiol 2009;20:S538-44.
26. Miyayama S, Yamashiro M, Hashimoto M, Hashimoto N, Ikuno M, Okumura K, Yoshida M, Matsui O. Identification of small hepatocellular carcinoma and tumor-feeding branches with cone-beam CT guidance technology during transcatheter arterial chemoembolization. J Vasc Interv

© Quantitative Imaging in Medicine and Surgery. All rights reserved.

Radiol 2013;24:501-8.
27. Lal H, Singh RKR, Yadav P, Yadav A, Bhadauria D, Singh A. Non-contrast MRA versus contrast enhanced MRA for detection of renal artery stenosis: a comparative analysis in 400 renal arteries. Abdom Radiol (NY) 2021;46:2064-71.

Cite this article as: Chiang LH, Chen YC, Huang GS, Huang TF, Sun YC, Chang WC, Hsu YC. Efficacy and reliability of three-dimensional fusion guidance for fluoroscopic navigation in transarterial embolization for refractory musculoskeletal pain. Quant Imaging Med Surg 2023;13(12):7719-7730. doi: 10.21037/qims-23-490

© Quantitative Imaging in Medicine and Surgery. All rights reserved.